

## Computational Study of a Doping-Less Tunneling CNTFET with Drain Work Function Engineering for the Improvement of the On/Off Current Ratio

Maryam Ghodrati

Department of Electronics, Faculty of Engineering, Lorestan University, Khorram-Abad, Iran; ghodrati.ma@fe.lu.ac.ir

### Abstract

In this work, a new structure based on a doping-less tunneling CNTFET using the drain work function engineering is presented. In the proposed structure, the drain electrode is divided into two parts with different work functions. The drain work function adjacent to the channel is selected higher than the other part of the drain. The results show that the proposed structure reduces the off-state current and increases the on/off current ratio. Also, the leakage current and the sub-threshold swing are significantly reduced. The computational study of the proposed structure has been done by quantum simulation using the non-equilibrium Green's function (NEGF).

**Keywords:** doping-less tunneling CNTFET, current ratio, off current, non-equilibrium green's function (NEGF).

### Introduction

Carbon nanotubes (CNTs) are a good alternative to silicon substitutes in transistors due to their properties such as one-dimensional nature, high mobility, adjustable band gap, symmetrical valence and conduction bands, high strength, and high thermal and electrical conductivity. On the other hand, due to their small diameter, their controllability by the gate is higher [1-7]. In order to overcome the quantum limitations and build integrated circuits with low energy consumption, various devices such as tunneling CNTFETs have been provided. These devices have received great attention due to their low off-state current and low sub-threshold swing compared to MOSFETs [6-18]. In recent years, numerous experimental and theoretical researches have been reported to improve the performance of tunneling CNTFETs in terms of scaling capability and figure of merits. These include the use of hetero-dielectric dual material gate doping-less TFET [2], junction-less work function engineered gate [9, 19], the combination of high-k and low-k gate dielectric technique [7], and various structures based on electrostatic doping have been proposed [20-25]. In this regard, a doping-less tunneling CNTFET has been introduced using the drain work function engineering. In the proposed structure, the drain electrode is divided into two parts with different work functions. The drain work function adjacent to the channel is selected higher than the other part of the drain. A comparison has been made between the proposed structure and the conventional tunneling CNTFET with the same dimensions. The simulations of the structures have been performed in the ballistic regime using the

non-equilibrium Green's function (NEGF) approach in the mode space.

### Device Structure and Simulation Method

Figure 1 shows the proposed doping-less tunneling CNTFET and the conventional tunneling CNTFET. The nanotube is a zigzag type (13, 0) with a diameter of 1 nanometer. The gate dielectric insulation of HfO<sub>2</sub> has 2 nm thickness and dielectric constant equals to 16. In the proposed structure, the drain electrode is divided into two parts with different work functions. The work function of the area adjacent to the channel is selected higher than the other part of the drain. The length of the drain (source) is 30 nm, the length of the gate is equal to the length of the channel equal to 20 nm. The physical specifications of the proposed structures is described in Table 1.

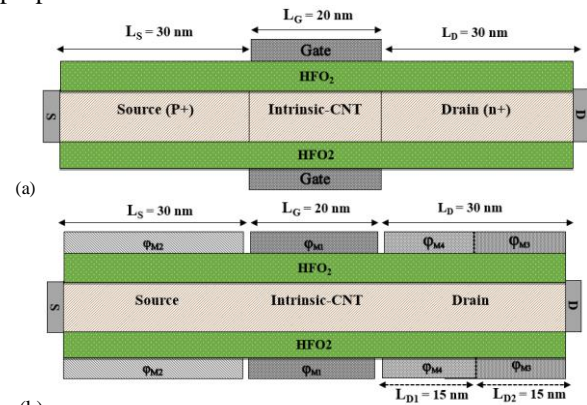


Figure 1. Cross-sectional view of (a) the conventional tunneling CNTFET (b) the proposed doping-less tunneling CNTFET.

Table 1. Physical parameters of the proposed structure.

Parameters	Proposed structure
CNT type	zigzag (13,0)
CNT diameter	1 nm
Gate length	20 nm
Drain length	30 nm ( $L_{D1} = 15\text{nm}$ , $L_{D2} = 15\text{nm}$ )
Source length	30 nm
Gate work function	$\phi_{M1} = 4.4\text{eV}$
Drain work function	$\phi_{M4} = 3.9\text{eV}$ , $\phi_{M3} = 3.4\text{eV}$
Source work function	$\phi_{M2} = 5.4\text{eV}$

In this paper, the numerical modeling of the Schrodinger equation using the non-equilibrium Green's function approach is used self-consistently by the Poisson equation. The CNT channel and the coupling of the nanotube into the drain and source regions are described by the Hamiltonian (H) matrix and self-energy matrices

$\sum_1$  and  $\sum_2$ , respectively. The Green's function is calculated as follows [1, 8, 21, 22]:

$$G(E) = [(E + i0^+)I - H - \sum_1 - \sum_2]^{-1} \quad (1)$$

Given Green's function, the desired physical parameters can be obtained using NEGF formulation. In the ballistic regime, the states of the channel are filled by the Fermi level of the source and the drain, which are calculated by the following equation [1, 8, 21, 22]:

$$D_{1(2)} = G\Gamma_{1(2)}G^+ \quad (2)$$

where,  $\Gamma_{1(2)}$  represents the flattening of energy levels due to the source and drain connections, which is determined as follows [1, 8, 21, 22]:

$$\Gamma_{1,2} = i(\sum_{1,2} - \sum_{1,2}^\dagger) \quad (3)$$

In the next step, the charge distribution inside the channel can be determined based on the states filled by the source and drain connections. The charge density in the channel using the Green's function is determined as follows [1, 8, 21, 22]:

$$Q_c = (-e) \int_{E_1}^{\infty} (D_S f(E - E_{FS}) + D_D f(E - E_{FD})) dE \quad (4)$$

where,  $e$  is the charge of the electron,  $E_{FS}$  and  $E_{FD}$  are the Fermi levels of source and drain. To solve the self-consistent, the NEGF equation is repeatedly solved by the Poisson equation until the self-consistent is obtained. After the self-consistent is reached, the current is calculated using the following equation [1, 8, 21, 22]:

$$I = \frac{4e}{h} \int T(E) [f_1(E) - f_2(E)] dE \quad (5)$$

where,  $T(E)$  is the transfer coefficient between the source and the drain which is calculated as follows [1, 8, 21, 22]:

$$T(E) = \text{trace}(\Gamma_1 G \Gamma_2 G^+) \quad (6)$$

All simulation results presented in here have been performed using MATLAB software.

## Results and Discussion

The drain current curve versus the drain-source voltage for the proposed structure, and the conventional tunneling CNTFET is shown in figure 2.

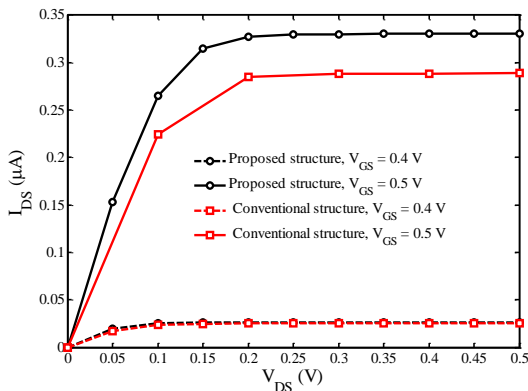


Figure 2.  $I_{DS}$ - $V_{DS}$  curve for proposed structure and conventional structure in  $V_{GS} = 0.4$  and  $0.5V$ .

It can be seen that in the given gate-source voltages, the saturation current for the proposed structure is less than the conventional tunneling CNTFET. The on-state current at voltage  $V_{GS} = 0.5V$  for the proposed structure is  $0.29 \mu A$  and for the conventional structure is  $0.33 \mu A$ . In figure 3, the drain current curve versus gate-source voltage is examined. It can be seen that in the proposed structure, the off-state current is significantly reduced compared to the conventional tunneling CNTFET. In the proposed structure using the drain work function engineering, the tunneling barrier at the drain-channel connection is widened. As a result, the off-state current for the proposed structure in  $V_{DS} = 0.2V$  and  $V_{GS} = 0V$  is about six times smaller than the conventional tunneling CNTFET.

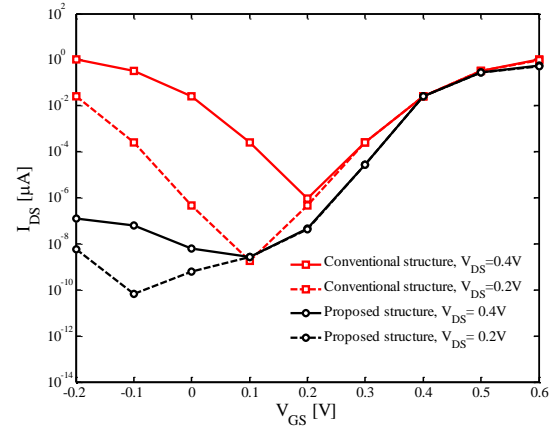


Figure 3.  $I_{DS}$ - $V_{GS}$  curve for the proposed structure and conventional structure in  $V_{DS} = 0.2, 0.4V$ .

One of the most important phenomena in the study of short channel effects is the sub-threshold swing (SS). The sub-threshold swing is determined by the following formula [1, 8, 21, 22]:

$$SS = 10^3 \frac{V_{GS2} - V_{GS1}}{\log(I_{DS2}) - \log(I_{DS1})} \text{ (mV/dec)} \quad (7)$$

The curve of the sub-threshold swing versus gate-source voltage is shown in figure 4.

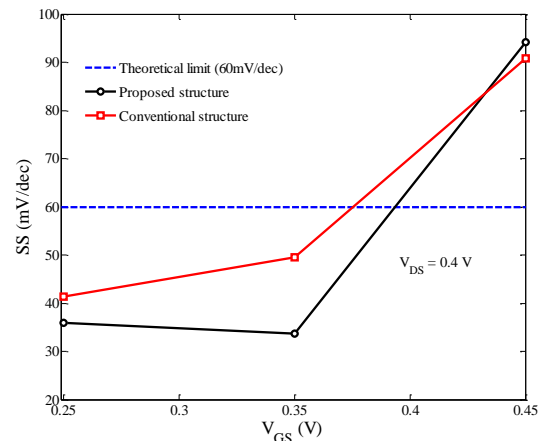


Figure 4. Sub-threshold swing versus  $V_{GS}$  for the proposed structure and conventional structure at  $V_{DS} = 0.4 V$ .

As can be seen, the sub-threshold swing of the proposed structure is significantly improved compared to the conventional tunneling CNTFET. The sub-threshold swing at the  $V_{DS} = 0.4$  V and  $V_{GS} = 0.3$  V voltages for the proposed structure is  $SS = 34.82$  mV/decade while for the conventional structure is  $SS = 45.45$  mV/decade. The sub-threshold swing decrease in the proposed structure is due to the widening of the tunneling barrier in the drain-channel connection.

The on/off current ratio curve is plotted versus the on-state current in figure 5. It can be seen that the on/off current ratio at  $V_{DS} = 0.4$  V for the proposed structure is higher than the conventional structure.

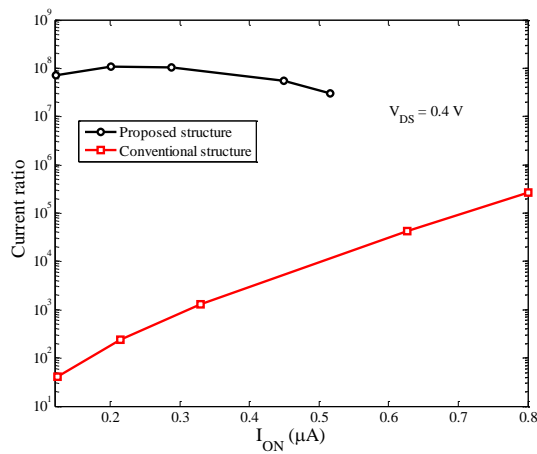
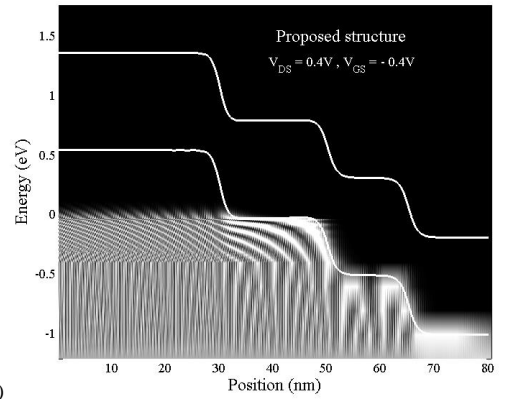


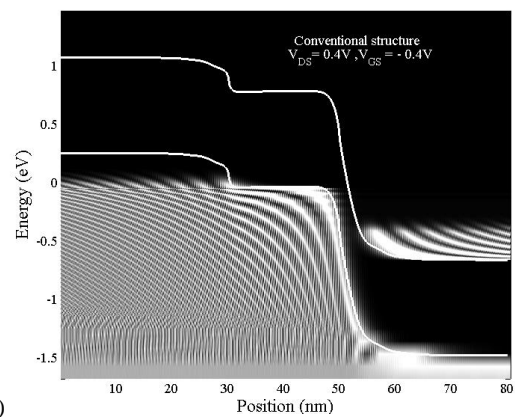
Figure 5. Current ratio versus  $I_{ON}$  for the proposed structure and conventional structure in  $V_{DS} = 0.4$  V.

The maximum current ratio is larger than  $10^8$  ( $I_{on}/I_{off} > 10^8$ ) for the proposed structure while for the conventional structure is larger than  $10^5$  ( $I_{on}/I_{off} > 10^5$ ). The on/off current ratio of the proposed structure has a significant increase compared to the conventional structure, which is due to the reduced curvature of the band near the drain-channel connection and the narrowing of the tunneling path in the OFF zone.

Figure 6 shows the energy band diagram versus position along the device in  $V_{GS} = -0.4$  V and  $V_{DS} = 0.4$  V. According to results, the distance between the conduction and valance bands at the channel-drain junction in the proposed structure is greater than the conventional tunneling CNTFET, so the probability of the band to band tunneling in the proposed structure at negative gate-source voltages is much lower. The proposed doping-less tunneling CNTFET, with dual electrodes with different work functions along the drain region, reduces the curvature of the band near the drain-channel connection and widens the tunneling barrier and improves the ambipolar behavior than the conventional tunneling CNTFET.



(a)



(b)

Figure 6. Energy band diagram versus position along the device at  $V_{DS} = 0.4$  V and  $V_{GS} = -0.4$  V for (a) the proposed structure and (b) the conventional structure.

Table 2 shows the results of the comparison between some of the performance parameters for the proposed doping-less tunneling CNTFET, and the conventional structure.

Table 2. Comparison between some of the performance parameters for the proposed and conventional structures.

Parameters	Proposed	Conventional
On-current ( $\mu A$ )	$2.88 \times 10^{-1}$	$3.30 \times 10^{-1}$
Off-current ( $\mu A$ )	$2.74 \times 10^{-9}$	$2.50 \times 10^{-4}$
On/Off current ratio	$1.05 \times 10^8$	$1.30 \times 10^5$
SS (mV/dec)	34.82	45.45

## Conclusions

In this paper, a new structure based on a doping-less tunneling CNTFET was proposed using drain work function engineering and the electrical properties of the device are simulated using the NEGF approach. The simulation results indicate that the performance of the proposed structure compared to the conventional structure has better using the drain work function engineering. The high on/off current ratio, and the low sub-threshold swing are among the advantages of the proposed structure.

## References

- [1] S. Datta, 2000, Nanoscale device modeling: the Green's function method, *Superlattices Microstruct.* 28 (2000) 253–278.
- [2] S. Anand, S. Intekhab Amin and R.K. Sarin, 2017, "Performance Analysis of different material based Dual Electrode Doping-less TFET", *European Advanced Materials Congress*, vol. 6, no. 2, pp. 384-387.
- [3] M. S. Ram and D. B. Abdi, 2015, "Doping less PNP Tunnel FET with Improved Performance: Design and Analysis," *Superlattices Microstruct.*, vol. 82, PP. 430-437.
- [4] M. Ghodrati, A. Mir, A. Farmani, 2020, Carbon nanotube field effect transistors-based gas sensors. *Nanosensors for Smart Cities*, Elsevier, 2020, pp. 171–183.
- [5] J. M. Marulanda. *Carbon Nanotubes* (In-Tech Press, India, 2010).
- [6] M. Ghodrati, A. Farmani, and A. Mir, 2019, "Nanoscale sensor-based tunneling carbon nanotube transistor for toxic gases detection: A first-principle study," *IEEE Sensors J.*, 19(17), Sep, pp. 7373–7377.
- [7] S. H. Tahaei, S. S. Ghoreishi, R. Yousefi, and H. Aderang, 2019, "A computational study of a carbon nanotube junctionless tunneling field-effect transistor (CNT-JLTFET) based on the charge plasma concept," *Superlattices Microstruct.*, vol. 125, pp. 168–176.
- [8] M. Ghodrati, A. Mir, and A. Naderi, 2020, "New structure of tunneling carbon nanotube FET with electrical junction in part of drain region and step impurity distribution pattern," *AEU-Int. J. Electron. Commun.*, 117, 153102.
- [9] B. Ghosh and M. W. Akram, 2013, "Junctionless Tunnel Field Effect Transistor," *IEEE Electron Device Lett.*, Vol. 34, No.5, pp.584-586.
- [10] M. Ghodrati, A. Mir, A. Naderi, 2021, "Proposal of a doping-less tunneling carbon nanotube field-effect transistor", *Mater. Sci. Eng. A: B.*, 256.
- [11] A. Naderi et al., 2017, "Improving band-to-band tunneling in a tunneling carbon nanotube field effect transistor by multi-level development of impurities in the drain region", *Eur. Phys. J. Plus.* vol.132 p.510, 107397.
- [12] A. Naderi et al., 2020, "The use of a Gaussian doping distribution in the channel region to improve the performance of a tunneling carbon nanotube field-effect transistor", *J Comput. Electron.*, vol. 19, pp. 283-290.
- [13] C. Qiu, Z. Zhang, M. Xiao, Y. Yang, D. Zhong, and L.-M. Peng, 2017, "Scaling carbon nanotube complementary transistors to 5-nm gate lengths," *Science*, vol. 355, no. 6322, pp. 271–276, doi: 10.1126/science.aaj1628.
- [14] M. Ghodrati, A. Mir, A. Farmani, 2022, "Sensitivity-Enhanced Surface Plasmon Resonance Sensor with Bimetal/ Tungsten Disulfide (WS<sub>2</sub>)/MXene (Ti<sub>3</sub>C<sub>2</sub>T<sub>x</sub>) Hybrid Structure", *Plasmonics* 17, 1973–1984.
- [15] A. Naderi et al., 2018, "An efficient structure for T-CNTFETs with intrinsic-n-doped impurity distribution pattern in drain region", *Turk J. Electr. Eng.*, vol. 26, pp. 2335 – 2346.
- [16] A. Naderi et al., 2018, "Cut off Frequency Variation by Ambient Heating in Tunneling p-i-n CNTFETs", *ECS J. Solid State Sci. Technol.*, vol. 7, pp. M6-M10.
- [17] A. M. Ionescu, and H. Riel, 2011, "Tunnel field-effect transistors as energy efficient electronic switches," *Nature*, Vol. 479, PP. 329-337.
- [18] M. Ghodrati, A. Mir, A. Farmani, 2022, "Proposing of SPR biosensor based on 2D Ti<sub>3</sub>C<sub>2</sub>T<sub>x</sub> MXene for uric acid detection immobilized by uricase enzyme", *J Comput Electron.*, <https://doi.org/10.1007/s10825-022-01959-w>.
- [19] Y. Lv, Q. Huang, H. Wang, S. Chang, and J. He, 2016, "A numerical study on graphene nanoribbon heterojunction dual-material gate tunnel FET," *IEEE Electron Device Lett.*, vol. 37, no. 10, pp. 1354–1357.
- [20] M. Ghodrati, A. Mir, A. Farmani, 2021, "Non-destructive label-free biomaterials detection using tunneling carbon nanotube-based biosensor", *IEEE Sens. J.*, vol. 21, pp. 8847-8854.
- [21] S. O. Koswatta, M. S. Lundstrom, D. E. Nikonov, 2009, "Performance comparison between p-i-n tunneling transistors and conventional MOSFETs" *IEEE Trans Electron Devices*, 56(3): 456-465.
- [22] M. Ghodrati, A. Mir, 2022, "Improving the Performance of a Doping-Less Carbon Nanotube FET with Dual Junction Source and Drain Regions: Numerical Studies", *J. Circuits Syst. Comput.*, doi.org/10.1142/S0218126622501821.
- [23] S. Bala and M. Khosla, 2018, "Design and analysis of electrostatic doped tunnel CNTFET for various process parameters variation," *Superlattices Microstruct.*, vol. 124, pp. 160–167, doi: 10.1016/j.spmi. 2018.10.007.
- [24] M. Ghodrati, A. Mir, A. Farmani, 2023, "Numerical analysis of a surface plasmon resonance based biosensor using molybdenum disulfide, molybdenum trioxide, and MXene for the diagnosis of diabetes", *Diam. Relat. Mater.*, vol. 132, 109633.
- [25] C. Sahu and J. Singh, 2014, "Charge-plasma based process variation immune junctionless transistor," *IEEE Electron Device Lett.*, vol. 35, no. 3, pp. 411–413.